Digital Object Identifier: 10.1109/ULTSYM.2008.0301

A new photoacoustic method for measuring optical transport Green's functions in turbid media

Roger J. Zemp, Xuhui Chen, Huihong Lu, Yan Jiang, & Kory Mathewson,
Department of Electrical & Computer Engineering
University of Alberta
Edmonton, Alberta, Canada
zemp@ece.ualberta.ca

***Abstract*—Photoacoustic imaging has shown great promise as a hybrid imaging technique offering optical contrast and ultrasonic spatial resolution. The optical contrast in photoacoustic images is primarily due to optical absorption rather than optical scattering, yet optical scattering is a tissue parameter of key importance. Here a new photoacoustic method for estimating the optical scattering properties of tissues is presented. The technique is based on the idea that the ultrasonic focal region of a transducer is an effective virtual detector of relative laser fluence, and translocation of light relative to the fixed ultrasound focus will provide an effective measure of the Green's function of radiative light transport in tissues. A novel light delivery probe was created and tested to prove the concept of the idea.**

Keywords-photoacoustic imaging, optical scattering, biomedical optics, high-frequency ultrasound

I. INTRODUCTION

Photoacoustic imaging is a novel hybrid imaging technique combining contrast advantages of optical methods with the spatial resolution of ultrasound imaging [1]. Recently, photoacoustic imaging has been used to visualize optically absorbing structures such as microvessels in vivo with high spatial resolution [2-4] and has been shown to have significant potential for functional [5] and molecular imaging [6, 7]. While sensitive to optical absorption, photoacoustic imaging has unfortunately thus far provided little information about tissue optical scattering properties. Yet, the optical scattering coefficient is an important tissue parameter which may reveal significant information about multiple diseases. Additionally, current photoacoustic reconstruction methods of blood oxygen saturation estimation suffer from unknown wavelength-dependent laser fluences, which could be in part remedied should optical scattering properties of tissue be known. While other optical methods have been used to measure optical scattering coefficients, to date we know of no photoacoustic method to do so.

We propose a new method for measuring the optical scattering coefficients of tissue based on the photoacoustic effect. We consider the photoacoustic signal source from a subcutaneous absorbing structure as an effective optical fluence detector below the surface of the skin. The basic premise behind our proposed technique involves transmitting a small area laser spot on the surface of the tissue, and to localize a small blood vessel via photoacoustic methods. While the ultrasound focus is fixed on the vessel, the light spot is laterally translated across the tissue surface. In a homogeneous turbid media, the received photoacoustic amplitude as a function of light-spot translation distance is an effective measurement of the optical Green's function for radiative transport. By fitting this Green's function estimate to models of light transport, we hypothesize that we can quantitatively estimate the mean optical absorption and optical reduced scattering coefficient of the tissue.

II. METHODS

A. Probe Design

To realize the aforementioned measurement technique with a reflection-mode geometry, a unique experimental design is required as present photoacoustic light-delivery techniques are not suitable for translocation of a small light spot. We require a method to deliver a focused light spot confocally with ultrasound, yet require the flexibility to translate the light spot relative to the ultrasound focus. A unique photoacoustic probe has been designed and fabricated for this purpose.

A key enabling aspect to the probe design is the delivery of a laser beam through a fused quartz prism to the sample area as shown in Fig. 1. Optical index matching fluid enables the light to propagate undeflected to the sample area. A focused ultrasound transducer faces the downward-45^{o} face of the prism, causing an effective ultrasound focus confocal with the light beam. Additional optics allowed for focusing and translation of the light, enabling the desired reflection-mode measurement technique we desire. Lens L1 was used for focusing the laser light such that the focal spot was of minimum diameter at the tissue or phantom surface. Lens L2 was chosen to have a radius of curvature such that each optical ray of the focused beam would hit a locally normal surface so as to prevent index-induced path deflection. The laser beam, and lenses L1 & L2 were translated together via a translation stage to laterally translate the incident light spot.

Index-matching fluid was purchased from Cargille-Labs, which possessed an optical index of refraction of 1.46, matching that of the fused silica prism. While the optical index-of-refraction of the fluid was well-known, what was not known was the acoustic properties of the fluid. Ideally the

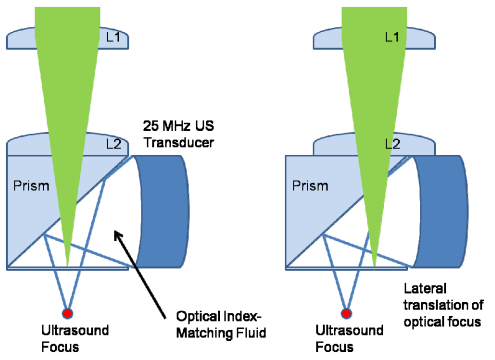

Figure 1. Illustration of our photoacoustic probe and how it may be used to measure optical scattering properties of tissues. The Lens L1 is used to focus a laser beam. The curvature of lens L2 is such that each light ray of the focused light beam is normal to its surface. Optical index matching fluid is used so that the focused beam will not be deflected by the prism. The prism, however, will deflect ultrasound to and from the focused ultrasound transducer.

fluid will have a speed of sound & acoustic impedance similar to that of soft tissue or water (~1.5MRayl) to prevent reflections or distortions at the fluid-tissue boundary. Additionally, we want the acoustic impedance of the optical index-matching fluid to be quite different than the prism to ensure that virtually no acoustic energy is transmitted into the prism. Finally we desire minimal acoustic attenuation. Optical index-matching oil was also measured but found to have a very high acoustic attenuation, and thus was not considered further.

We measured the acoustic attenuation and speed of sound of the index matching fluid. This was accomplished by using a 25-MHz focused ultrasound transducer to measure the pulse-echo delay as a function of the translated distance of a steel reflector plate immersed in the fluid. The slope of the resulting plot indicated the speed of sound of the fluid. The acoustic impedance was found from the product of the measured speed of sound and the known fluid density of the fluid. Our measurement results are displayed in Table 1, along with data for water and fused silica (quartz). Fortuitously, we measured the speed of sound in the index-matching fluid as only 4-5% less than that of water and only ~3% less than – and within error of the speed of sound of tissue. Due to a low density, however, the acoustic impedance (1.2 MRayl) is ~20% less than that of tissue – meaning that acoustic reflections at the tissue-fluid interface will occur, however, this is only a small loss, and some loss due to the membrane isolating the index-matching fluid from the tissue will be expected anyways. The

Table 1. Physical properties of index-matching fluid compared with water and fused quartz.

	Speed (km/s)	Attenuation (dB/cm at 25 MHz)	Density (g/cc)	Acoustic Impedance	Optical Index of Refraction
Water	1.51 ± 0.03	1.38± 0.02	0.997 ± 0.001	1.51 ± 0.03	1.333
Index Liquid	1.44 ± 0.04	2.7 ± 0.1	0.831± 0.001	1.20 ± 0.03	1.46
Fused Quartz	5.98	0.006	2.2	13	1.46

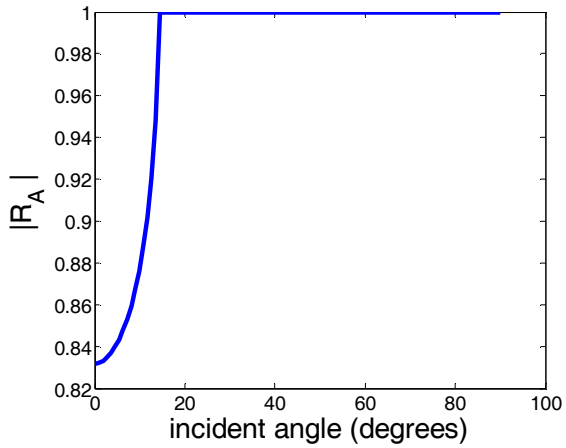

Figure 2. Computed acoustic reflection coefficient of ultrasound at a fused silica – index-matching fluid interface, as a function of incident ultrasound angle.

low acoustic impedance of the fluid is advantageous for reflection of ultrasound from the prism's diagonal face. We compute that above a critical angle of ~16° ultrasound incidence (as measured from the normal to the prism surface), 100% of the incident ultrasound will be reflected while no ultrasound will propagate into the prism. This is illustrated in the computed curve of reflection coefficient amplitude as a function of incident angle, shown in Fig. 2.

In the current probe design, we use a transducer with a 6-mm active aperture and a 12.7-mm focus, corresponding to an F-number of 2.1. The transducer has an additional 2-mm steel housing corresponding to a transducer diameter of 10-mm. We use a 10-mm prism, and the prism and transducer are housed in a custom-machined acrylic holder. 2-mm of fused silica was ground off of one edge of the prism to allow the transducer active element to be as close to the top edge of the prism's oblique face as possible, giving as deep a focal depth as possible. Our current focal depth as measured from the bottom of our probe is ~3mm – which is comparable with the penetration depth of present photoacoustic microscopy systems. A 25-micron plastic membrane (Saran Wrap ©) was fixed to the bottom of the probe using specialized double-sided tape, to hold the index matching fluid. In the future a mechanical seal with an O-ring may be considered.

Figure 3. Photograph of the photoacoustic imaging system used in our laboratory.

B. *Photoacoustic Imaging System*

We needed to test the efficacy of the new light delivery system for photoacoustic imaging, and we conducted phantom-based spatial-resolution studies to do so. We mounted our probe on a voice-coil actuator stage (H2W technologies). The voice-coil stage is capable of 15-Hz oscillations, corresponding to 30-imaging frames per second in a scanned imaging mode, but for the current experiments, the frame-rate was limited by the 10-20-Hz pulse repetition rate of the laser. A servo-controller was programmed to take a step for each laser pulse, scanning up to 1" with steps as small as 5 microns. A pulsed Nd:YAG laser pulsing 7-8ns pulses of 532-nm light of up to 9 mJ (however, we used <1mJ) in a 1.5-mm radius beam was used as the optical excitation source. An ultrasound receiver with 40dB of gain was used to amplify the received signal. A photograph of the system is shown in Fig. 3.

III. RESULTS

A. *Point-Spread Function Measurements*

Fig. 4 shows a number of point-spread functions as a function of depth. These point-spread functions were acquired by imaging a human hair at varying depths and superimposing the 7 images. In this photoacoustic imaging mode, the transducer, prism, lenses, and beam are scanned together across the hair phantom. Focal resolution is quantified as ~250x40microns. No distortions due the probe design were observed.

B. *Optical Scattering Measurements*

The mode for measuring optical scattering curves is different than the photoacoustic imaging mode. Here, after localizing the probe over the water-immersed hair (by maximizing the received signal using pulse-echo ultrasound), the laser beam was aligned to hit the hair, maximizing the photoacoustic signal. This procedure ensures that the laser is aligned confocally with the ultrasound axis. At this stage, the light was then laterally translocated as described above. A manual translation stage was used for this purpose. The

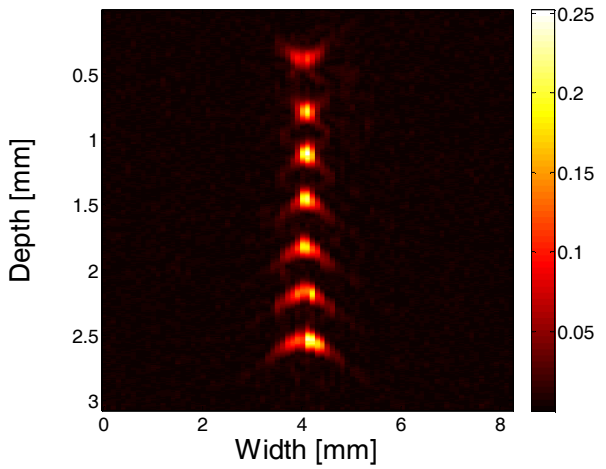

Figure 3. Photoacoustic microscopy composite image of hair-fibers at different depths. The colormap represents received volts after 39dB amplification.

This work was was sponsored by the Terry Fox Foundation through the National Cancer Institute of Canada (NCIC TFF 019237 & 019249), NSERC (G121211115), & the Alberta Cancer Board (ACB 23728).

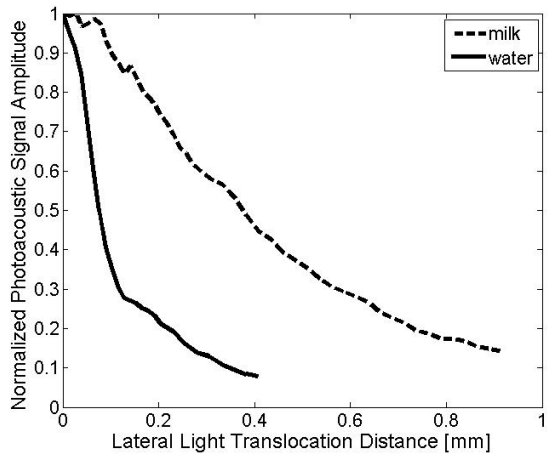

Figure 2. Photoacoustic signal magnitude as the ultrasound transducer focus is fixed on a hair target, while the illumination spot is laterally translated. The curve is broader for milk (blue curve) compared with water (black curve), as milk has a higher optical scattering coefficient.

received photoacoustic signal magnitude was plotted as a function of light translocation distance. As expected, with only a hair in the water, the photoacoustic signal drops rapidly after moving only ~100 microns (the approximate distance of the hair width). After doing this experiment with only a hair in water, evaporated milk was added to the water to impart optical scattering properties similar to 2% milk. We then repeated the light translocation experiment. Even when the light-spot is translated ~1mm from the origin, the hair still experiences laser fluence due to optical scattering, and produces a broader curve, as shown in Fig. 5.

IV. DISCUSSION

The light spot size was measured by taking a burn profile using photographic paper and measured ~200 microns in diameter (but improvements in the spot shape are warranted for future work). The estimated fluence is ~300mJ/cm^2, which is higher than the ANSI limit, but lower than the ~6mJ/cm^2 used for FDA-approved laser treatments. Lower fluences are certainly possible at the expense of signal-to-noise and addition of averaging. Using a ring-shaped illumination, and expanding the ring diameter may serve the same purpose as translocating a light spot, but with the advantage of spreading out the laser pulse energy over a wider area and reducing the laser fluence while keeping the same effective pulse energy delivery. This will be considered for future work.

The present technique offers an effective measurement of the Green's function of the optical transport from a surface location to a subsurface location. Knowledge of this Green's function may potentially be a very powerful tool for quantitative photoacoustic microscopy. In future work we will fit these measured curves with modeled curves of radiative transport, and an optimization procedure should produce estimates of the mean optical scattering coefficients of biological tissues. We must account for the finite beam-spot size and finite ultrasound focal volumes when doing this. Knowing the surface laser fluence, we can then predict the

subsurface laser fluence at a desired location. This will be important for quantitative estimation of blood oxygenation and molecular imaging, where unknown wavelength-dependent fluences are presently unknowns in estimation algorithms, and may be a source of measurement artifacts.

Knowledge of radiative transport Green's functions may also play a role in reconstruction algorithms for photoacoustic data. Present techniques such as molecular fluorescent tomography [8] use a multiplicity of sources and a multiplicity of detectors on the surface of a subject. While many source-detector pairs are potentially possible, many of these measurements are degenerate, and the reconstruction algorithms are ill-posed. With the present technique, we are effectively introducing more potential detectors (photoacoustic virtual detectors) below the surface, which may provide information for reconstruction algorithms in a less degenerate way than is currently possible.

It is also worthwhile to note that the proposed method is currently employed to take measurements in the radiative transport regime (<3mm depths in tissue) rather than the diffusion regime. The transport-regime below the quasi-balistic regime of traditional microscopy and optical coherence imaging techniques represents a realm of considerable difficulty for optical imaging, and few techniques can perform measurements using a reflection-mode geometry in this regime. We envision techniques similar to [9, 10] for transport-regime image reconstruction of optical absorption and scattering parameters.

V. Conclusions

We have demonstrated a new photoacoustic measurement technique which shows promise for determining optical scattering coefficients of biological tissues. A unique photoacoustic probe was shown to be an enabling technology for these measurements to be made.

Acknowledgment

We are grateful to Prof. Robert Fedosejevs for lending us the Nd:YAG laser used in this article.

References

[1] M. H. Xu and L. H. V. Wang, "Photoacoustic imaging in biomedicine," *Review of Scientific Instruments,* vol. 77, Apr 2006.

[2] E. Zhang and P. Beard, "Broadband ultrasound field mapping system using a wavelength tuned, optically scanned focused laser beam to address a Fabry Perot polymer film sensor," *IEEE Transactions on Ultrasonics Ferroelectrics and Frequency Control,* vol. 53, pp. 1330-1338, Jul 2006.

[3] K. Maslov, G. Stoica, and L. V. H. Wang, "In vivo dark-field reflection-mode photoacoustic microscopy," *Optics Letters,* vol. 30, pp. 625-627, Mar 15 2005.

[4] H. F. Zhang, K. Maslov, M. L. Li, G. Stoica, and L. H. V. Wang, "In vivo volumetric imaging of subcutaneous microvasculature by photoacoustic microscopy," *Optics Express,* vol. 14, pp. 9317-9323, Oct 2 2006.

[5] H. F. Zhang, K. Maslov, G. Stoica, and L. H. V. Wang, "Functional photoacoustic microscopy for high-resolution and noninvasive in vivo imaging," *Nature Biotechnology,* vol. 24, pp. 848-851, Jul 2006.

[6] A. De La Zerda, C. Zavaleta, S. Keren, S. Vaithilingam, S. Bodapati, Z. Liu, J. Levi, B. R. Smith, T. J. Ma, O. Oralkan, Z. Cheng, X. Y. Chen, H. J. Dai, B. T. Khuri-Yakub, and S. S. Gambhir, "Carbon nanotubes as photoacoustic molecular imaging agents in living mice," *Nature Nanotechnology,* vol. 3, pp. 557-562, Sep 2008.

[7] L. Li, R. J. Zemp, G. Lungu, G. Stoica, and L. H. V. Wang, "Photoacoustic imaging of lacZ gene expression in vivo," *Journal of Biomedical Optics,* vol. 12, pp. -, Mar-Apr 2007.

[8] E. E. Graves, J. Ripoll, R. Weissleder, and V. Ntziachristos, "A submillimeter resolution fluorescence molecular imaging system for small animal imaging," *Medical Physics,* vol. 30, pp. 901-911, May 2003.

[9] A. Dunn and D. Boas, "Transport-based image reconstruction in turbid media with small source-detector separations," *Optics Letters,* vol. 25, pp. 1777-1779, Dec 15 2000.

[10] E. M. C. Hillman, D. A. Boas, A. M. Dale, and A. K. Dunn, "Laminar optical tomography: demonstration of millimeter-scale depth-resolved imaging in turbid media," *Optics Letters,* vol. 29, pp. 1650-1652, Jul 15 2004.